

Article

The Influences of Adsorption Mechanism of Linear and Branched Alkanes Liquid Contacting Face-Centered Cubic Lattice on Heat Transport

Abdul Rafeq Saleman^{1,*}, Nazri Md Daud¹, Mohd Nizam Sudin¹, Mohammad Shukri Zakaria¹, Mohd Afzanizam Rosli¹, Fudhail Abdul Munir² and Bukhari Manshoor³

¹ Faculty of Mechanical Technology and Engineering, Universiti Teknikal Malaysia Melaka, Durian Tunggal, Melaka, 76100, Malaysia

² Department of Mechanical Engineering, Faculty of Engineering, Universiti Teknologi Petronas, Bandar Seri Iskandar, Perak, 32610, Malaysia

³ Faculty of Mechanical and Manufacturing Engineering, Universiti Tun Hussein Onn Malaysia, Batu Pahat, Johor, 86400, Malaysia

* Correspondence: rafeq@utem.edu.my;

Received: 30 July 2024; **Revised:** 14 August 2024; **Accepted:** 16 September 2024; **Published:** 11 November 2024

Abstract: In tribology studies, the interaction between solid and liquid surfaces is a common focus, with particular attention given to wear rates and surface scars. These wear and scar issues are analyzed through adsorption mechanisms. A key factor in these problems is the orientation of the liquid on solid surfaces, which requires an in-depth examination of molecular orientations. This study aims to investigate the adsorption mechanisms of liquids on solid surfaces by analyzing structural quantities such as density, orientation order parameters and radius of gyration. The research employs molecular dynamics simulations to model a gold solid with face-centered cubic (FCC) (100) surfaces in contact with three different alkanes (pentane, heptane, and 3-ethylpentane). The simulations are conducted at a uniform temperature set at 0.7 of the liquid's critical temperature. It is found that, in all the structural quantities, high adsorption behavior have been observed near the solid surfaces. And among these three liquids, 3-ethyl-pentane exhibit the lowest value of adsorption behavior. Results indicate that liquids with linear molecular structures exhibit higher adsorption behavior compared to those with branched structures, which in a way will affects heat transfer near the contact interfaces. Further research is needed to explore how the surface structure of the solid affects these interactions with different types of liquid with branches.

Keywords: Solid-Liquid Interfaces; Adsorption Mechanism; Alkane Liquid; Molecular Dynamics Simulations.

1. Introduction

Solid-liquid interfaces where solid surfaces come into contact with long-chain polymers play a critical role in various technological and biological applications. These include thermal interface materials [1], energy systems [2], tri-

biological systems [3], NEMS and MEMS technology [4], and many more. Understanding the equilibrium and non-equilibrium properties of these interfaces at the nanoscale is essential for advancing our knowledge of nanoscale materials. When the thickness of polymeric films approaches the nanometer scale, traditional macroscopic theories and physics become inadequate. In these nanoscale systems, interface behaviors are primarily influenced by molecular interactions at the solid-liquid interface and the surface morphology of the solid [1,5], which can be described through adsorption mechanisms. Knowledge of adsorption mechanisms is fundamental to understanding phenomena such as adhesion [6], corrosion resistance [7,8], and lubrication [8], and is closely tied to the transport properties related to heat and mass transfer.

Previous research has explored adsorption mechanisms through studies of liquid adsorption on solid surfaces [1,5,9] and the effects of surface morphology [10,11]. However, despite extensive investigations, a detailed molecular-level understanding of liquid lubricants on solid surfaces remains lacking. This paper aims to address this gap by examining adsorption mechanisms from the perspective of molecular orientation on solid surfaces using non-equilibrium molecular dynamics simulations. Specifically, the study evaluates three types of alkane liquids (pentane, 3-ethyl-pentane, and heptane) in contact with a Face-Centered Cubic (100) surface, assessing adsorption mechanisms based on density, orientation order parameter, and radius of gyration.

2. Methods

2.1. Model and Simulation Basic Dimensions

The simulation establishes a system organized in a structured, layered configuration consisting of alternating solid, liquid, and solid phases, as depicted in Figure 1. In this setup, the interfaces where the solid and liquid phases come into contact are referred to as solid-liquid (S-L) interfaces. Consequently, this system features two distinct S-L interfaces within its arrangement. The solid phase in the simulation is represented by a gold surface with a face-centered cubic (FCC) crystal structure with the (100) plane, which interacts with three different liquid substances namely are pentane, 3-ethyl-pentane, and heptane.

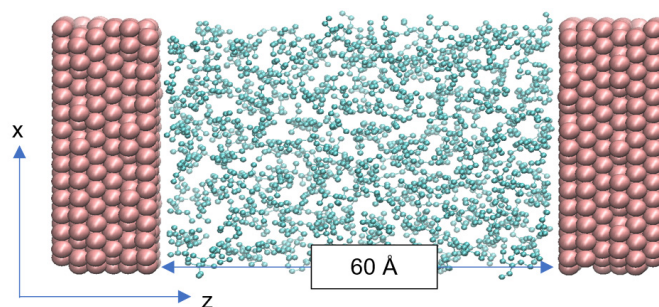


Figure 1. Layered arrangement of solid, liquid and solid of the simulation system

The dimensions of the overall simulation system are $40.7 \text{ \AA} \times 40.7 \text{ \AA} \times 114.4 \text{ \AA}$ along the x, y, and z directions, respectively. The details of the number of liquid molecules for pentane, 3-ethylpentane and heptane is tabulated in **Table 1** along with the number of solid atoms in x, y and z-directions. Within this setup, the liquid layer extends to a length of 60 \AA in the z-direction in between the layers of solid. To model the behavior of an infinitely large solid, periodic boundary conditions are applied in the x and y directions, allowing for continuous replication of the system in these directions. In contrast, the z-direction is constrained to remain fixed at its position, thereby simulating the conditions of an extensive and unbounded solid extending infinitely to the left and right. This configuration aims to replicate and investigate the interactions and properties at the solid-liquid interfaces as they would occur in a realistically large-scale system.

Table 1. Number of liquid molecules and number of solid atom in x, y and z-direction.

	Number of liquid molecules	Number of solid atoms in x, y and z
Pentane	445	10 × 20 × 6
Heptane	339	10 × 20 × 6
3-ethylpentane	336	10 × 20 × 6

2.2. Attraction and repulsion forces of solid and liquid

In order, to accurately model the behavior of solid and liquid phases within the simulation, a range of interaction forces must be meticulously applied to replicate real-world conditions. Specifically, the simulation addresses three main categories of interaction forces: solid-to-solid interaction forces, liquid-to-liquid interaction forces, and solid-to-liquid interaction forces. These forces are implemented based on established methods detailed in references [9,12,13], which provide the theoretical foundations and parameters necessary for the accurate representation of these interactions in the simulation. The solid-to-solid interaction forces are modeled by Morse potential which are given as in equation (1).

$$\Phi(r_{ij}) = D[e^{-2\alpha(r_{ij}-r_0)} - 2e^{-\alpha(r_{ij}-r_0)}] \quad (1)$$

where D is the constant interaction forces between solid atoms given as 7.6148×10^{-13} erg, r_0 is the equivalent distance between solid atoms is 3.0242 Å and alpha is 1.5830 Å⁻¹ [14,15].

In particular, the liquid-to-liquid interaction forces are modeled using two primary types of forces: bonded interaction forces and non-bonded interaction forces. The bonded interaction forces encompass three distinct types of interactions essential for simulating the internal dynamics of liquid molecules. These include stretching interactions, which resist changes in bond lengths between atoms; bending interactions, which resist changes in the angles between bonds; and torsion interactions, which account for the resistance to rotational movements around bonds. These bonded forces are crucial for accurately representing the structural properties and flexibility of liquid molecules. The bonded interaction consists of inter-molecular interactions which calculate the forces of CH₂-to-CH₂, and CH₂-to-CH₃ interaction forces. The CH₂ and CH₃ are represented as pseudo atom in this study, the details explanation related to the pseudo atom are elaborated in refs [5,17]. The bonded interaction which are stretching interactions are given as equation (2).

$$U(r_{ij}) = \frac{k_r}{2}(r_{ij} - b_{eq})^2 \quad (2)$$

where the k_r is energy value of the interaction between inter-molecules of liquid given as 1.3323×10^{-19} j/rad and b_{eq} is 1.54 Å. The bending interactions is given by equation (3).

$$U(\theta) = \frac{k_\theta}{2}(\theta - \theta_0)^2 \quad (3)$$

where k_θ and θ_0 is given in Table 2. And finally the torsion interaction which is given as equation (4).

$$U(\varphi) = V_0 + V_1(1 + \cos \varphi) + V_2(1 - \cos 2\varphi) + V_3(1 + \cos 3\varphi) \quad (4)$$

Where the detail value of each parameter is shown in **Table 3**

Table 2. Bending Interaction Parameters.

	θ_0	$k\theta/kB$
Pentane & Heptane	114.00°	62500 K
3-ethylpentane	109.47°	62500 K

¹ kB is boltzman constant (1.3806×10^{-23}).

Table 3. Torsional Interaction Parameters.

	V_0/kB (K)	V_1/kB (K)	V_2/kB (K)	V_3/kB (K)
Pentane & Heptane	0	355.04	-6819	791.32
3-ethylpentane	1416.3	398.3	139.12	901.2

¹ kB is boltzman constant (1.3806×10^{-23}).

Alongside bonded forces, the non-bonded interaction forces are also employed to represent the interactions that occur between molecules or between different parts of the same molecule that are not directly connected by bonds. These non-bonded interactions primarily include Van der Waals forces, which consist of attractive forces between molecules or atoms separated by more than two bond lengths. Van der Waals forces, which include London dispersion forces and dipole-dipole interactions, are fundamental for capturing the cohesive behavior of liquids. The methods for modeling these non-bonded forces follow the approaches outlined in references [17] and [18], which utilized the Universal Force Fields (UFF) given as equation (5).

$$U^{LJ}(r_{ij}) = 4\epsilon_{ij} \left[\left(\frac{\sigma_{ij}}{r_{ij}} \right)^{12} - \left(\frac{\sigma_{ij}}{r_{ij}} \right)^6 \right] \quad (5)$$

The r_{ij} is the distance between the atom i and j . The σ_{ij} and ϵ_{ij} is calculated by the Lorent-Bertholet combining rules to calculates the interaction forces given as equation (6) and equation (7).

$$\epsilon_{ij} = \sqrt{\epsilon_{ii}\epsilon_{jj}} \quad (6)$$

and

$$\sigma_{ij} = \frac{\sigma_{ii} + \sigma_{jj}}{2} \quad (7)$$

For the solid-to-liquid interaction forces, the simulation utilizes the Lorentz-Bertholet combining rules. These rules provide a systematic approach to calculate the cross-interaction parameters between the solid and liquid phases, ensuring that the interactions at the solid-liquid interface are realistically represented. The use of the Lorentz-Bertholet combining rules in this study adheres to the techniques described in references [9] and [1], which offer a robust framework for these types of interfacial interactions.

2.3. Simulation Step

In molecular dynamics simulation the data that is crucial to collect is the velocity and position of each molecule. In this study, the velocity and position data are calculated by the reversible reference propagator algorithm (R-RESPA). The r-RESPA calculate the velocity and position based on the forces of the inter-molecular and intra-molecular interactions respectively for 1 femto second and 0.2 femto second.

Initially the simulation system is run at 0 K for 10000-to-30000-time step for liquid molecules and solid atom to be in an equilibrium positions. Then the simulation system temperature was raised slowly to the 0.7 of the critical

temperature of the liquids. After the simulation system reached the temperature, it is maintained at the temperature for 1-million-time step. This step is to make sure the simulation system has uniform temperature of 0.7 of the critical temperature. Then finally, the data collection step, where the simulation system is run for another 2-million-time step.

3. Results

3.1. Distribution of Density in z-Direction

In order to understand the character of the adsorption behavior of liquid on solid surface the density distribution of the system of layer of solid liquid solid is tabulated. To calculate the density distributions the simulation systems was divided into 5900 slabs with the thickness of approximately 0.02 Å in the z-direction.

Figure 2 illustrates the density distributions of the simulation models for Pentane, Heptane and 3-ethyl-pentane in contact with FCC (100). This distribution reveals characteristic features that have been observed in prior research studies [1,5,12,13], where a notable oscillation is present near the solid surfaces on both sides of the simulation system and a relatively constant density is found in the central region of the distribution. The constant value at the central region of the density distribution is used to validate the simulation model. The value should have approximately the same value of the liquid at the 0.7 of the critical temperature of the liquid. Based on the central region of the density distribution it is found that all three liquid is validated, and the value is approximately 570 kg/m³ for pentane [19], 610 kg/m³ for heptane [20] and 622 for 3-ethyl-pentane [21]. As depicted in Figure 2 there exists oscillation closest to the solid surfaces. This kind of oscillation is referred to as the adsorption layer of liquid.

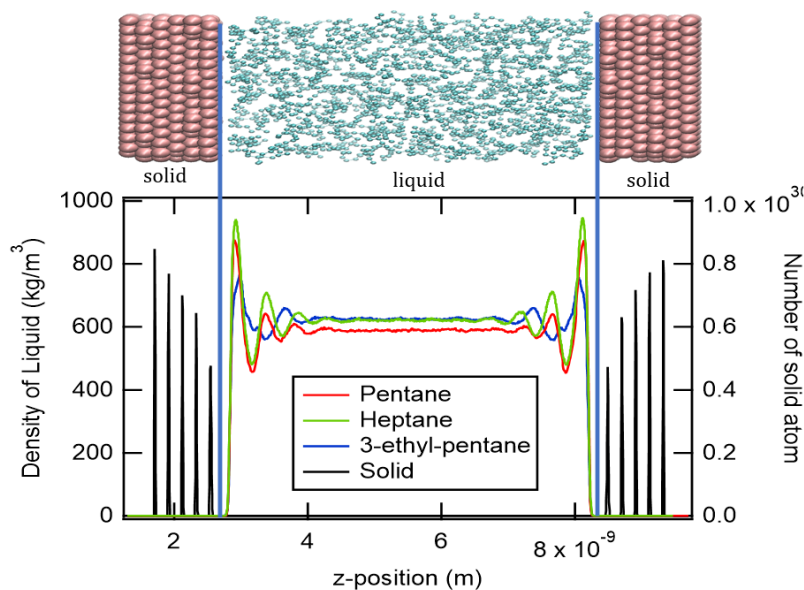


Figure 2. Density distributions of pentane, 3-ethyl-pentane and heptane.

Due to the inherent symmetry of the model, Figure 3 shows only the left half of the density distribution profiles is depicted in the figure for further analysis. The results show that the adsorption layers for heptane and pentane are both thicker and positioned closer to the solid surface compared to 3-ethyl-pentane. Specifically, the peak density of the adsorption layer for heptane is approximately 945.28 kg/m³, followed by pentane at 797.89 kg/m³, and 3-ethyl-pentane at 758.11 kg/m³. Additionally, the density distribution profile for 3-ethyl-pentane exhibits noticeable differences in the positions of the peaks and valleys compared to heptane and pentane. These variations arise from the differences in molecular structure among the liquids. While both pentane and heptane possess a linear molecular structure, 3-ethyl-pentane

features a branched structure at the center of the molecule. This branching introduces differences in the behavior of intermolecular forces, influencing the observed adsorption phenomena. The position of the peaks represents the adsorption behavior of each of the liquid. based on past investigations, it is understood that the closer the position of the adsorption layer shows the higher the adsorption of the liquid that may influences the shear rate of the liquid [22]. Additionally, the height of the peaks of the adsorption layer represents the force characteristics in which higher peaks shows higher heat transfer rate and adsorption force [9,13]. As established in previous studies [23], the oscillations observed near the solid surfaces are attributed to the interplay of attractive and repulsive forces between the liquid molecules and the solid surface. Based on the density distribution results, it is evident that heptane exhibits the highest level of adsorption onto the gold solid surface, followed by pentane, with 3-ethyl-pentane showing the least adsorption.

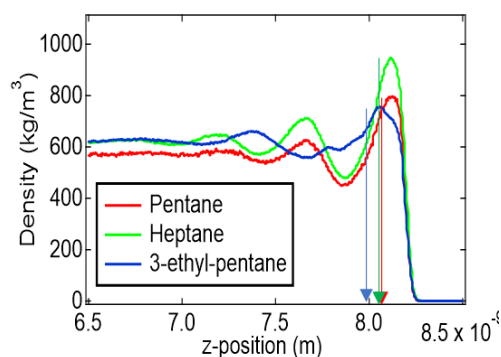


Figure 3. Density distributions of pentane, 3-ethyl-pentane and heptane.

3.2. Order Parameters

Orientation order parameters serve as a key reference metric for determining the alignment of liquid molecules relative to solid surfaces. This parameter is quantified on a scale from -0.5 to 1.0, where a value of -0.5 signifies that the liquid molecules are perfectly parallel to the solid surface, 1.0 indicates that the molecules are oriented perpendicular (normal) to the surface, and a value of 0 represents a completely random orientation of the molecules.

Figure 4 shows the Orientation Order parameter for pentane, Heptane and 3-ethyl-pentane imposed over the density of the liquid. The results displayed in the figure reveal that, near the solid surface, all three types of liquid exhibit a nearly parallel alignment. As the distance from the solid surface increases, the liquid molecules transition to a more normal orientation with respect to the surface. This pattern of behavior is consistent with findings from previous studies [5], which have also observed a shift from parallel to normal orientations as the distance from the solid surface increases towards the central region of the simulation system. As understood from previous studies [5,25,26] the central region does not have any influences from the solid surfaces thus the liquid does not have any influence on the orientation of the liquid does make it randomly oriented. For the case of the liquid near the solid surfaces the attraction force and repulsion forces from the solid surfaces that making the adsorptions layer of liquid in a way influences the orientation of liquid near the surfaces.

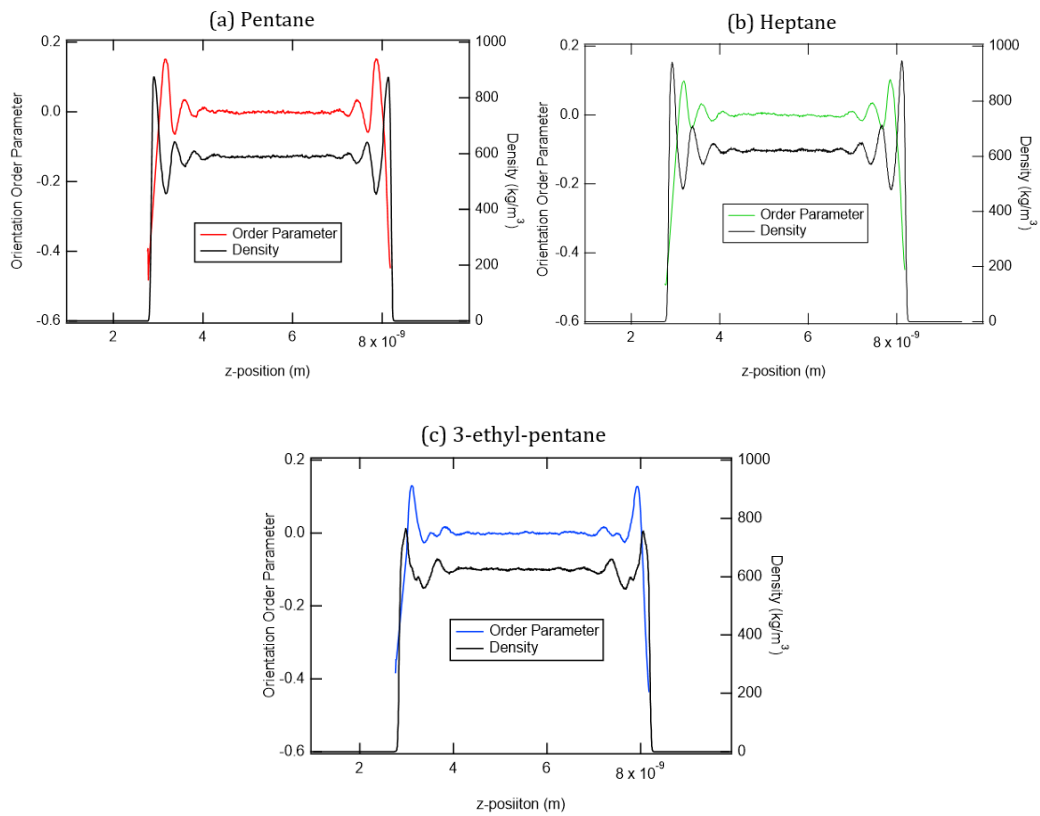


Figure 4. Orientation order parameter of (a) pentane, (b) Heptane and (c) 3-ethyl-pentane.

Figure 5 illustrates the orientation order parameters for pentane, 3-ethyl-pentane, and heptane, specifically for the left sides of the simulation model since as observed in Figure 4 it is symmetry. Based on **Figure 5**, there are noticeable differences in the profiles of the orientation order parameters among the different liquids. The figure shows that while the general shapes of the orientation profiles for heptane and pentane are quite similar, 3-ethyl-pentane exhibits some distinct variations. Specifically, the peaks and valleys in the orientation order parameter profile for 3-ethyl-pentane are less pronounced compared to those for heptane and pentane. This observation suggests that although 3-ethyl-pentane maintains a parallel orientation close to the solid surface, it is more prone to transitioning to a random orientation as the distance from the surface increases. This behavior highlights the greater stability of the parallel orientation for heptane and pentane compared to 3-ethyl-pentane.

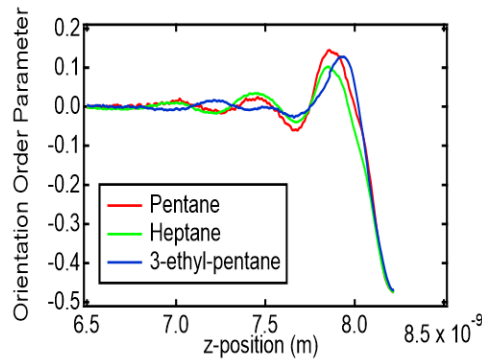


Figure 5. The left side of orientation order parameter of pentane, 3-ethyl-pentane and heptane super imposed between each other.

3.3. Radius of Gyration.

Radius of gyration is another structural quantity that have been utilized in the past to represent the characters of the liquid adsorption of solid surfaces [5,7]. The radius of gyration is an index that determines the shape of liquid. The radius of gyration is calculated by mean square given in equation (8).

$$R^2 = \frac{1}{N} \left\langle \sum_{i=1}^N (\vec{r}_i - \vec{r}_{cp})^2 \right\rangle \quad (8)$$

where N is the number of molecules in a slab, r is the position of each pseudo atom and r_{cp} is the center position the liquid molecules. In the present simulation in order to calculate the radius of gyration the simulation system was divided into 1200 number of slabs in the z-directions. Figure 6 shows the radius of gyration of pentane, 3-ethyl-pentane and heptane in a single plot. Based on the figure 3-ethyl-pentane has the lowest value of radius of gyration followed by pentane and the highest is heptane. As observed from the figure since the temperature of the simulation system is constant and on both sides of the simulation system present solid, the radius of gyration appear symmetry. This kind observation is similar to the past investigations [5,17]. Based on the previous investigation results the higher value of radius of gyration shows that the index of the shape of the liquid are in the parallel position with the solid. On the other hand, at the central region since the influence of the solid surface are not significant the index of the shape of the liquid are in randomly oriented.

Figure 7 shows the left sides of the radius of gyration for all three liquids. It is found that, for pentane and heptane there are a significant higher value of radius of gyrations appear near the solid surfaces, however such kind of presence does not observe for 3-ethyl-pentane. This observation suggests that the 3-ethyl-pentane is less significant to be adsorbed on the solid surfaces thus creating lower value of radius of gyration.

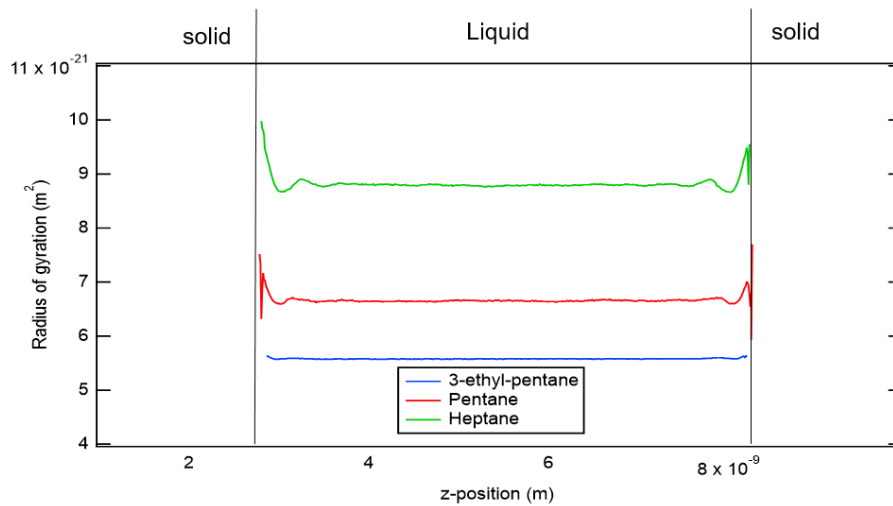


Figure 6.Radius of gyration of pentane, 3-ethyl-pentane and heptane super imposed between each other.

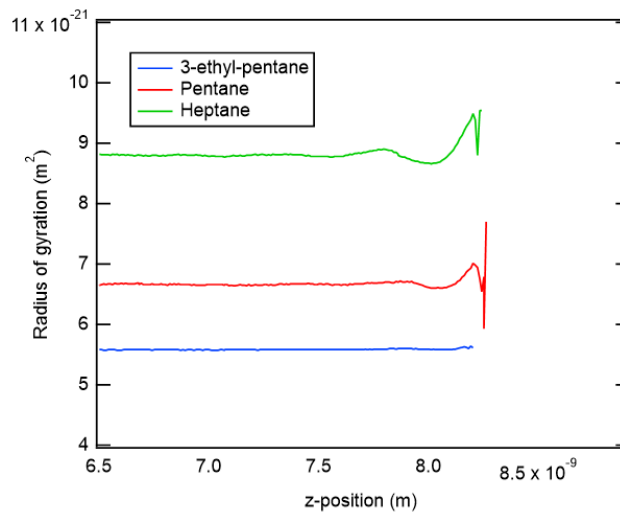


Figure 7.Left sides of the Radius of gyration for pentane, 3-ethyl-pentane and heptane super imposed between each other

4. Conclusions

This study examines the adsorption behavior of linear versus branched alkane liquids. It is found that, based on the structural quantities which are density, order parameter and radius of gyration, 3-ethyl-pentane is less likely to be absorbed on solid surfaces as compared to pentane and heptane. In overall, the findings indicate that branched liquids are less likely to adsorb onto solid surfaces compared to linear liquids. This difference significantly affects heat transfer at the solid-liquid interfaces and impacts hydrodynamic lubrication conditions. However in this investigation, the authors did not address different types of branched liquid such as different position of the branched liquid and longer branched liquid. In addition to that, this investigation only look at one types of Face-centered cubic (FCC) lattice surfaces of (100), although it is well known that FCC has 3 different types of surfaces namely are (100), (110) and (111). Thus, further research is needed to explore the effects of surface structure on contact interfaces, particularly for different FCC orientations such as (110) and (111) and also different types of branched liquid.

Author Contributions

Conceptualization, A. Rafeq S., M. Shukri Z., and M. Afzanizam M. R.; methodology, A. Rafeq S., Nazri M. D., and M. Shukri Z.; software, A. Rafeq S.; validation, M. Shukri Z., and Nazri M. D.; formal analysis, A. Rafeq S.; investigation, A. Rafeq S.; resources, A. Rafeq S.; data curation, M. Shukri Z. and M. Nizam S.; writing—original draft preparation, A. Rafeq S. and M. Shukri Z.; writing—review and editing, A. Rafeq S., M. Afzanizam M. R., M. Nizam S., and M. Shukri Z.; visualization, M. Shukri Z.; supervision, M. Afzanizam M. R., and Bukhari M.; project administration, A. Rafeq S.; funding acquisition, A. Rafeq S., M Shukri Z., M. Afzanizam M. R., and Bukhari M.. All authors have read and agreed to the published version of the manuscript.

Funding

This research was supported by Ministry of Higher Education of Malaysia grant number (FRGS/1/2022/TK05/UTEM/02/50).

Institutional Review Board Statement

Not applicable.

Informed Consent Statement

Not applicable.

Data Availability Statement

All data supporting the findings of this study are available and can be found in <https://figshare.com/s/fa9a127ebe5633702554>.

Acknowledgments

The authors gratefully acknowledge the funding from Ministry of Higher Education Malaysia (MOHE). Much appreciation also goes to the Universiti Teknikal Malaysia Melaka (UTeM) for allowing the numerical simulations to be performed on the Level 7th Computer Laboratory. The authors would like to thank Assoc. Prof. Gota Kikugawa from the Institute of Fluid Science, Tohoku University since he developed the software used to run the simulations.

Conflicts of Interest

The authors declare no conflict of interest.

References

1. A. R. bin Saleman, H. K. Chilukoti, G. Kikugawa, and T. Ohara, "A molecular dynamics study on the thermal rectification effect at the solid–liquid interfaces between the face-centred cubic (FCC) of gold (Au) with the surfaces of (100), (110) and (111) crystal planes facing the liquid methane (CH₄)," *Mol Simul*, vol. 45, no. 1, pp. 68–79, 2019, doi: 10.1080/08927022.2018.1535177.
2. J. M. G. Sousa, a. L. Ferreira, and M. a. Barroso, "Determination of the solid-fluid coexistence of the n - 6 Lennard-Jones system from free energy calculations," *Journal of Chemical Physics*, vol. 136, no. 2012, 2012, doi: 10.1063/1.4707746.
3. K. Holmberg and A. Erdemir, "Influence of tribology on global energy consumption, costs and emissions," *Friction*, vol. 5, no. 3, pp. 263–284, 2017, doi: 10.1007/s40544-017-0183-5.
4. L. Dai, N. Satyanarayana, S. K. Sinha, and V. B. C. Tan, "Analysis of PFPE lubricating film in NEMS application via molecular dynamics simulation," *Tribol Int*, vol. 60, pp. 53–57, 2013, doi: 10.1016/j.triboint.2012.10.021.
5. A. R. bin Saleman, H. K. Chilukoti, G. Kikugawa, M. Shibahara, and T. Ohara, "A molecular dynamics study on the thermal transport properties and the structure of the solid–liquid interfaces between face centered cubic (FCC) crystal planes of gold in contact with linear alkane liquids," *Int J Heat Mass Transf*, vol. 105, pp. 168–179, Feb. 2017, doi: 10.1016/j.ijheatmasstransfer.2016.09.069.
6. H. Al-Maliki, L. Zsidai, P. Samyn, Z. Szakál, R. Keresztes, and G. Kalácska, "Effects of atmospheric plasma treatment on adhesion and tribology of aromatic thermoplastic polymers," *Polym Eng Sci*, vol. 58, 2018, doi: 10.1002/pen.24689.
7. Y. Sun, "Surface Engineering & Coating Technologies for Corrosion and Tribocorrosion Resistance," Jul. 01, 2023, Multidisciplinary Digital Publishing Institute (MDPI). doi: 10.3390/ma16134863.
8. W. R. V. Sampaio et al., "Influence of using different titanium cathodic cage plasma deposition configurations on the mechanical, tribological, and corrosion properties of AISI 304 stainless steel," *Surf Coat Technol*, vol. 475,

- 2023, doi: 10.1016/j.surfcoat.2023.130149.
9. X. Liu et al., “A molecular dynamics study of thermal boundary resistance over solid interfaces with an extremely thin liquid film,” *Int J Heat Mass Transf*, vol. 147, p. 118949, 2020, doi: 10.1016/j.ijheatmasstransfer.2019.118949.
 10. T. Q. Vo, B. S. Park, C. H. Park, and B. H. Kim, “Nano-scale liquid film sheared between strong wetting surfaces: effects of interface region on the flow,” *Journal of Mechanical Science and Technology*, vol. 29, no. 4, pp. 1681–1688, 2015, doi: 10.1007/s12206-015-0340-6.
 11. D. T. Ta, A. K. Tieu, H. T. Zhu, and B. Kosasih, “Thin film lubrication of hexadecane confined by iron and iron oxide surfaces: A crucial role of surface structure,” *J Chem Phys*, vol. 143, no. 16, p. 164702, 2015, doi: 10.1063/1.4933203.
 12. A. Rafeq et al., “Comparison of the characteristic of heat transport between non-shear and shear systems at solid-liquid (S-L) interfaces,” no. May, pp. 270–272, 2018.
 13. A. R. Saleman et al., “Heat Transport at Solid-Liquid Interfaces between Face-Centered Cubic Lattice and Liquid Alkanes,” *Journal of Advanced Research in Fluid Mechanics and Thermal Sciences Journal homepage*, vol. 44, pp. 123–130, 2018, [Online]. Available: www.akademiabaru.com/arfmnts.html
 14. R. C. Lincoln, K. M. Koliwad, and P. B. Ghate, “Morse-potentials evaluations of second and third order elastic constants of some cubic metals,” *Phys Rev*, vol. 157, pp. 463–466, 1967, doi: <http://dx.doi.org/10.1103/PhysRev.157.463>.
 15. L. a. Girifalco and V. G. Weizer, “Application of the morse potential function to cubic metals,” *Physical Review*, vol. 114, no. 3, pp. 687–690, 1959, doi: 10.1103/PhysRev.114.687.
 16. H. K. Chilukoti, G. Kikugawa, and T. Ohara, “Structure and Mass Transport Characteristics at the Intrinsic Liquid-Vapor Interfaces of Alkanes,” *Journal of Physical Chemistry B*, vol. 120, no. 29, pp. 7207–7216, 2016, doi: 10.1021/acs.jpcc.6b05332.
 17. S. K. Nath and R. Khare, “New forcefield parameters for branched hydrocarbons,” *Journal of Chemical Physics*, vol. 115, no. 23, pp. 10837–10844, 2001, doi: 10.1063/1.1418731.
 18. H. Matsubara, G. Kikugawa, T. Bessho, S. Yamashita, and T. Ohara, “Effects of molecular structure on microscopic heat transport in chain polymer liquids,” *Journal of Chemical Physics*, 2015, doi: 10.1063/1.4919313.
 19. B. Le Neindre et al., “Thermal conductivity of gaseous and liquid n-pentane,” *Fluid Phase Equilib*, vol. 460, pp. 146–154, Mar. 2018, doi: 10.1016/j.fluid.2017.12.026.
 20. J. Ilja Siepmann and M. G. Martin, “Intermolecular potentials for branched alkanes and the vapour-liquid phase equilibria of n-heptane, 2-methylhexane, and 3-ethylpentane,” *Mol Phys*, vol. 90, no. 5, pp. 687–694, Apr. 1997, doi: 10.1080/002689797172048.
 21. H. Watanabe, “Thermal conductivity and thermal diffusivity of sixteen isomers of alkanes: C_nH_{2n+2} (n = 6 to 8),” *J Chem Eng Data*, vol. 48, no. 1, pp. 124–136, Jan. 2003, doi: 10.1021/je020125e.
 22. A. R. b. Saleman, H. K. Chilukoti, G. Kikugawa, M. Shibahara, and T. Ohara, “A molecular dynamics study on the thermal energy transfer and momentum transfer at the solid-liquid interfaces between gold and sheared liquid alkanes,” *International Journal of Thermal Sciences*, vol. 120, pp. 273–288, 2017, doi: 10.1016/j.ijthermalsci.2017.06.014.
 23. T. Ohara and D. Suzuki, “Intermolecular energy transfer at a solid-liquid interface,” *Microscale Thermophysical Engineering*, vol. 4, pp. 189–196, 2000, doi: 10.1080/10893950050148142.
 24. O. Kum, “Orientation effects in shocked nickel single crystals via molecular dynamics,” *J Appl Phys*, vol. 93, no. 6, pp. 3239–3247, 2003, doi: 10.1063/1.1554489.
 25. H. K. Chilukoti, G. Kikugawa, and T. Ohara, “Mass transport and structure of liquid n-alkane mixtures in the vicinity of α -quartz substrates,” *RSC Adv.*, vol. 6, no. 102, pp. 99704–99713, 2016, doi: 10.1039/C6RA22398B.



Copyright © 2024 by the author(s). Published by UK Scientific Publishing Limited. This is an open access article under the Creative Commons Attribution (CC BY) license (<https://creativecommons.org/licenses/by/4.0/>).

Publisher’s Note: The views, opinions, and information presented in all publications are the sole responsibility of the respective authors and contributors, and do not necessarily reflect the views of UK Scientific Publishing Limited and/or its editors. UK Scientific Publishing Limited and/or its editors hereby disclaim any liability for any harm or damage to individuals or property arising from the implementation of ideas, methods, instructions, or products mentioned in the content.